CHAPTER V
RESULTS AND DISCUSSION

5.1 Adsorption of Sulfur Compounds on NaX Zeolite

The sulfur compounds used were 3-metylthiophene (3MT) and benzothiophene (BT) for gasoline and dibenzothiophene (DBT) for diesel. Simulated transportation fuels used in this study were isooctane and decane to represent gasoline and diesel, respectively. Thus, the simulated fuels were prepared by mixing benzothiophene or 3-methylthiophene with isooctane to simulate gasoline and mixing dibenzothiophene with decane to simulate diesel.

5.1.1 Effect of Initial Concentration of Sulfur Compounds on Adsorption by NaX

In the adsorption process, the initial concentration of the solute plays important role. In this study, adsorption experiments using different initial concentrations of the model sulfur compounds were conducted in a continuous system. The initial concentrations of sulfur compounds in simulated transportation fuels were varied between 200 and 1800 ppmw. The results are shown in Figures 5.1 to 5.3 for 3-MT, BT and DBT, respectively. The Y axis represents effluent sulfur concentration normalized by the initial sulfur concentration and X axis represents treated fuel volume normalized by total bed weight. From the results, it can be observed that the change in the initial sulfur concentration has significant effect on breakthrough curve. At higher initial feed concentration, the slope of the breakthrough curve is steeper and the breakthrough time (treated volume) is shorter. The existence of a dynamic equilibrium of sulfur compounds between mobile phase and solid phase was considered. As the initial sulfur concentration in the feed increases, the adsorbent would be forced to adsorb much more sulfur compounds when compared to the lower sulfur concentration. Consequently, the change of concentration gradient affects the saturation rate and breakthrough time or in other words, the diffusion process is concentration dependent. Moreover, the length of the adsorption zone length decreases as the driving force for mass transfer increases.

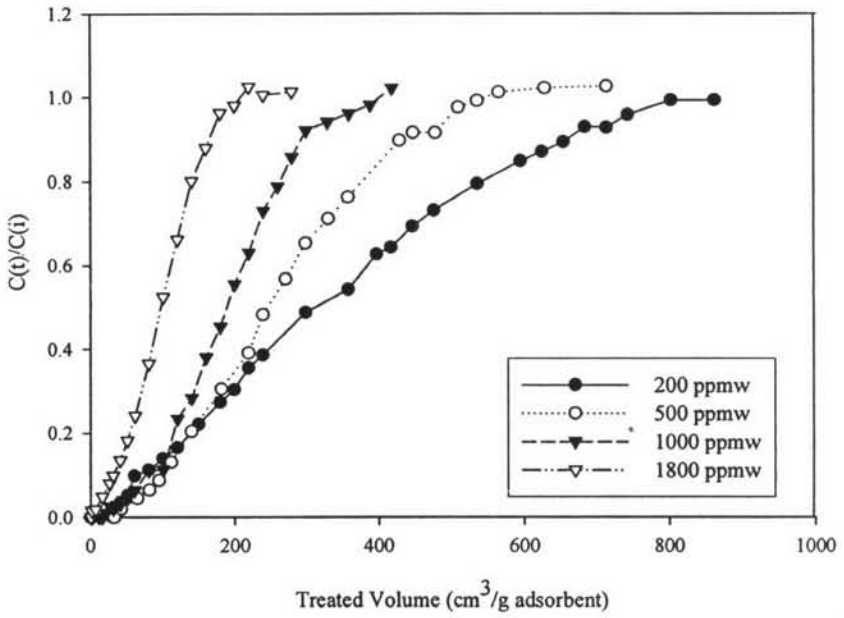

Figure 5.1 The effect of influent concentration of 3-methylthiophene on adsorption by NaX.

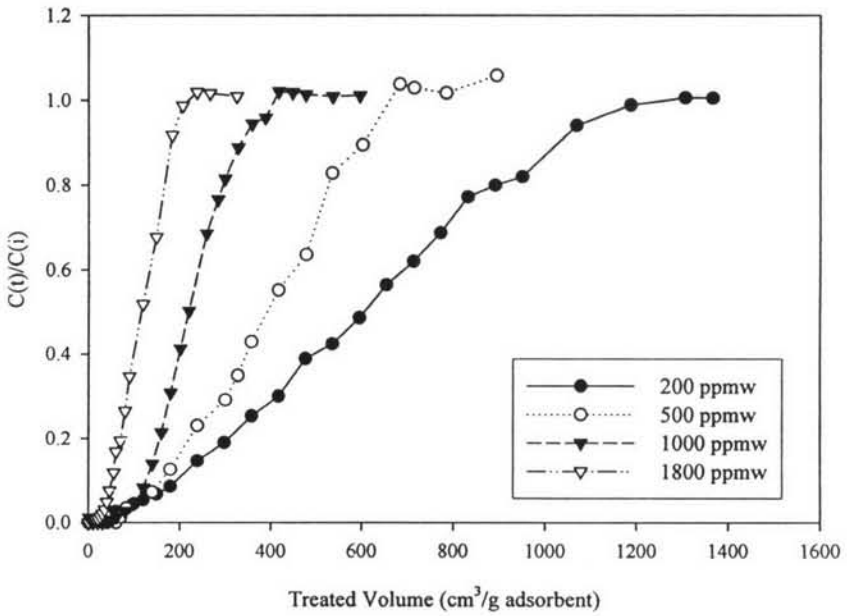

Figure 5.2 The effect of influent concentration of benzothiophene on adsorption by NaX.

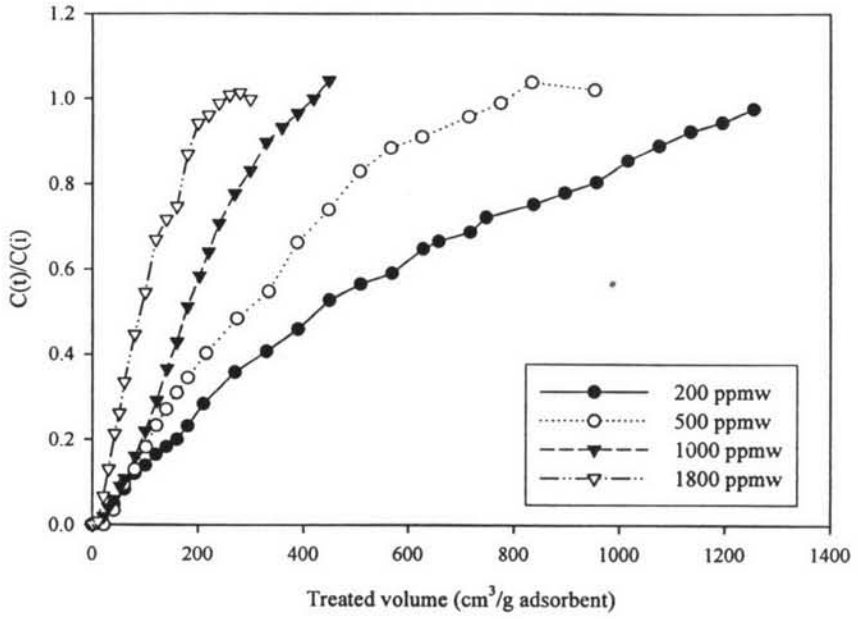

Figure 5.3 The effect of influent concentration of dibenzothiophene on adsorption by NaX.

5.1.2 Effect of Type of Sulfur Compounds on Adsorption by NaX

In this part of the study, the effect of type of sulfur compound in simulated transportation fuels on adsorption by NaX was studied. Figures 5.4 to 5.6 show the comparison between the adsorption of 3-MT, BT and DBT on NaX zeolites at 200, 1000, 1800 ppmw, respectively. The results show that the breakthrough point of three types of sulfur compound arranges in the order of BT>3-MT>DBT. The breakthrough point and shape of these curves appears to be strongly dependent on the size of sulfur molecule. In case of DBT that consists of two benzene rings in structure, it can be observed from the figure that the breakthrough point of DBT is the earliest due to the influence of steric hindrance effect on the adsorption of a relatively big molecule. For 3-MT and BT, the molecular size of 3-MT (5.9 °A) and BT (6.5 °A) is relatively small compared to the NaX zeolite's aperture (7.4 °A), and thus more 3-MT and BT can be adsorbed on NaX. This results in the slower breakthrough point of 3-MT and BT than DBT. It can be also seen that the breakthrough point of BT occurs slowest. This is attributed to the presence of benzene functional group in BT structure which can interact with zeolite acidic

surface via π-bonding (Yang *et al.*, 2001). The breakthrough and saturation capacities were calculated from the breakthrough curve and shown in the Tables 5.1 and 5.2. However, it was observed that the saturation capacities in continuous system were lower than those in batch system (Siriyut, 2005). This may be due to many factors effecting the continuous adsorption such as diffusion rate, contact time, etc.

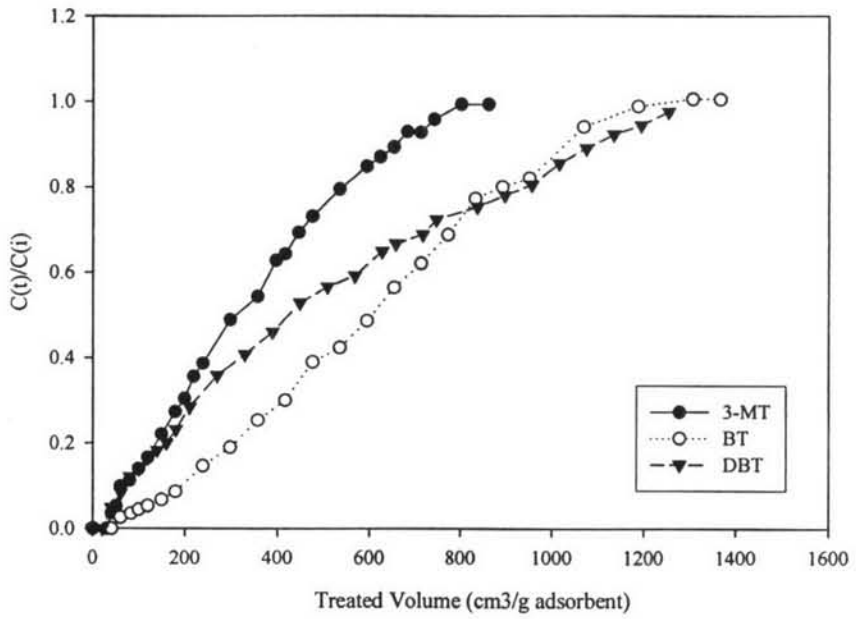

Figure 5.4 The effect of type of sulfur compounds at 200 ppmw on adsorption by NaX.

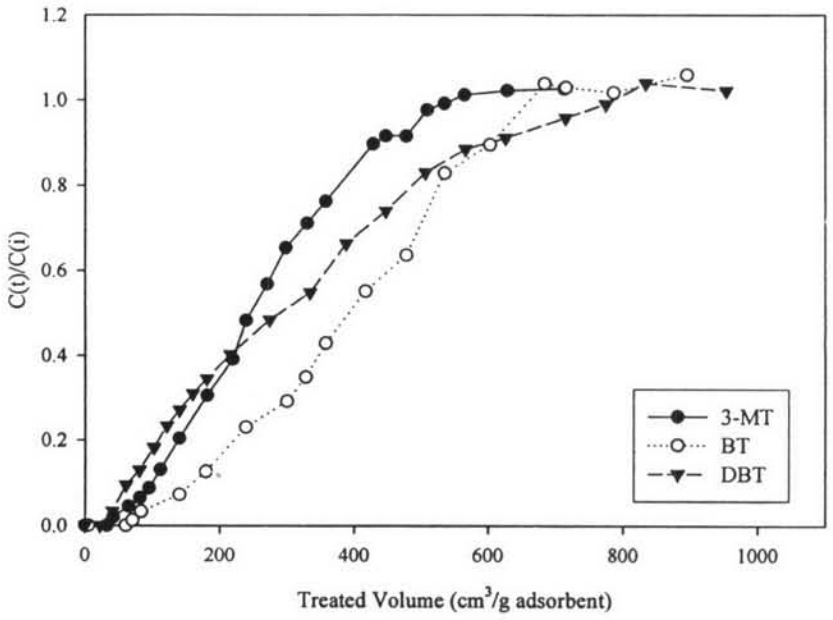

Figure 5.5 The effect of type of sulfur compounds at 500 ppmw on adsorption by NaX.

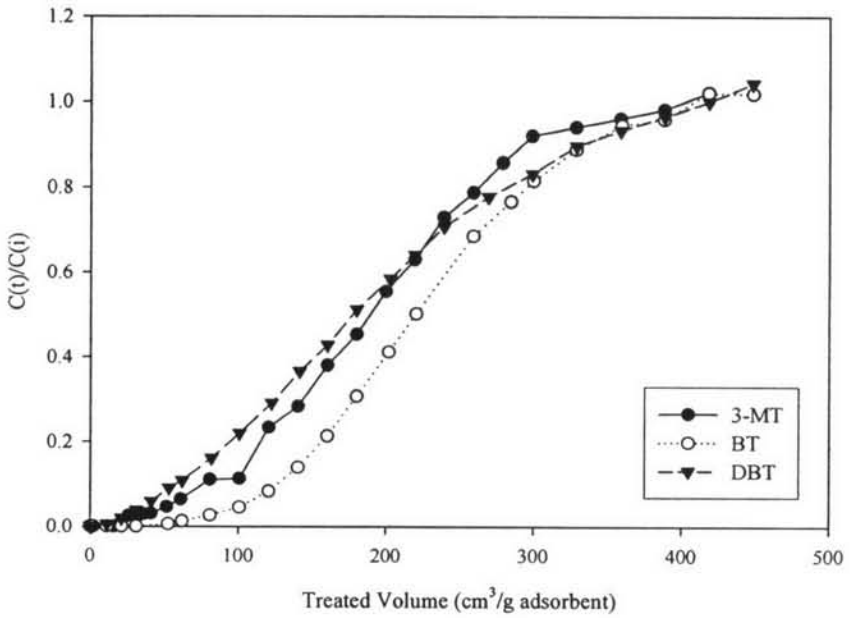

Figure 5.6 The effect of type of sulfur compounds at 1000 ppmw on adsorption by NaX.

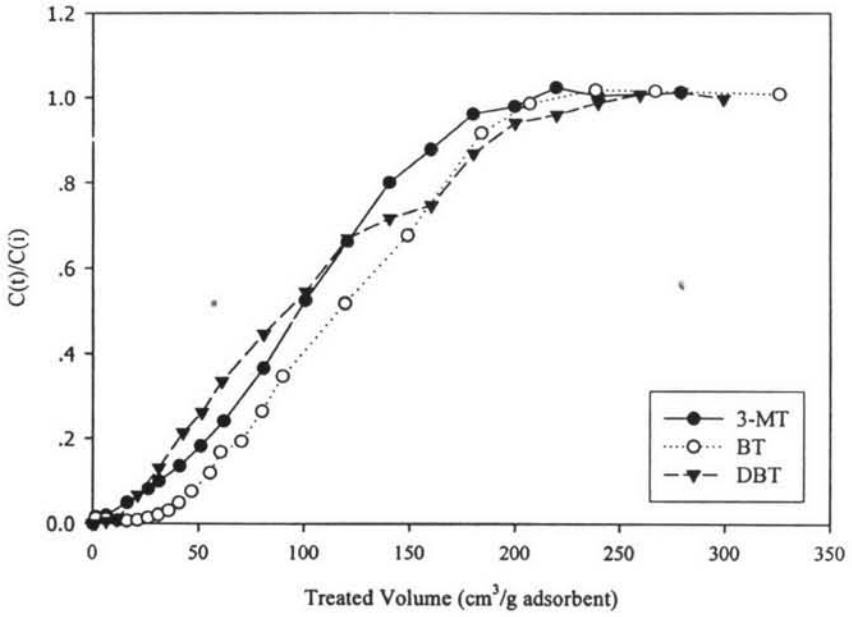

Figure 5.7 The effect of type of sulfur compounds at 1800 ppmw on adsorption by NaX.

Table 5.1 The breakthrough capacities of thiophenic sulfur compounds on NaX (5 ppmw)

Rank	Type of sulfur compounds	Breakthrough capacities (mmole g^{-1} adsorbent)			
		200 ppmw	500 ppmw	1000 ppmw	1800 ppmw
1	BT	0.07	0.17	0.27	-
2	3-MT	0.06	0.14	0.14	-
3	DBT	0.03	0.06	0.04	-

Table 5.2 The saturation capacities of thiophenic sulfur compounds on NaX (95% of initial sulfur concentration)

Type of sulfur compounds	Saturation capacities (continuous system) (mmole g^{-1} adsorbent)				Maximum capacities (batch system)
	200 ppmw	500 ppmw	1000 ppmw	1800 ppmw	
BT	0.71	0.96	1.26	1.25	1.34
3-MT	0.52	0.96	1.40	1.33	1.75
DBT	0.46	0.64	0.83	0.75	1.06

5.2 Desorption of Sulfur Compounds from Used Adsorbent by Heating Technique

In order to study the regeneration of the adsorbents, the desorption of the sulfur compounds adsorbed on NaX was studied by heating technique at 400°C to release the adsorbed sulfur compounds. Figures 5.8 and 5.9 show the comparison between the adsorption of 1000 ppmw of 3-MT on fresh NaX and regenerated NaX after heating column for 1 and 3 hours, respectively. The result shows that after the desorption of 3-MT adsorbed on NaX with nitrogen at 400°C for 1 hours, almost all of the original capacity of NaX can be recovered. The observed saturation capacity was approximately 1.05 mmol/g, which was 91.9% of the original capacity recovered. For 3 hours of heating column, NaX capacity can be recovered nearly the same amount (91.4%) of the original adsorption capacity. According to the insignificant difference in the recovered adsorption capacities between heating the column for 1 and 3 hours, it can be concluded that the heating time at 400°C for 1 hour is sufficient for full regeneration of NaX.

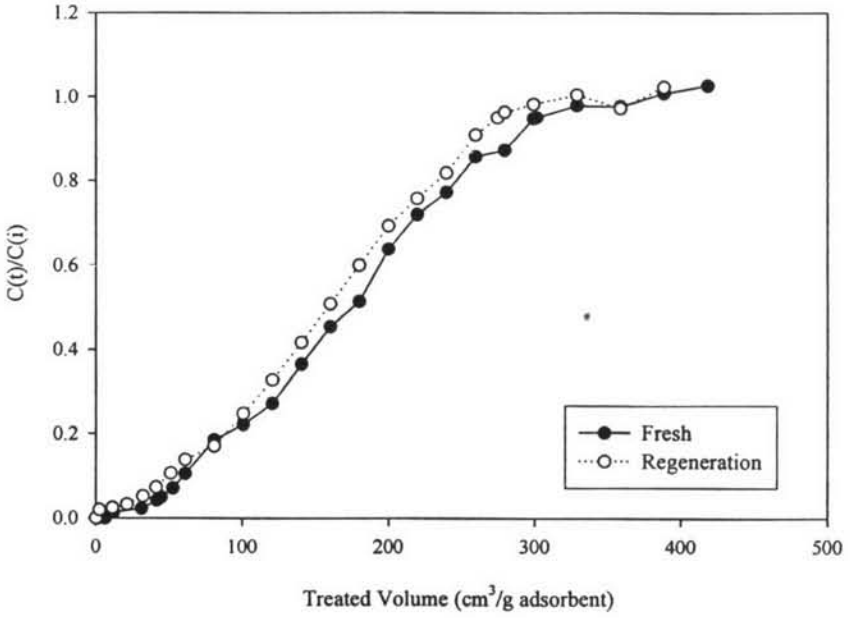

Figure 5.8 The effect of desorption of 3-methylthiophene by heating on NaX capacity (desorption time 1 hr at 400°C).

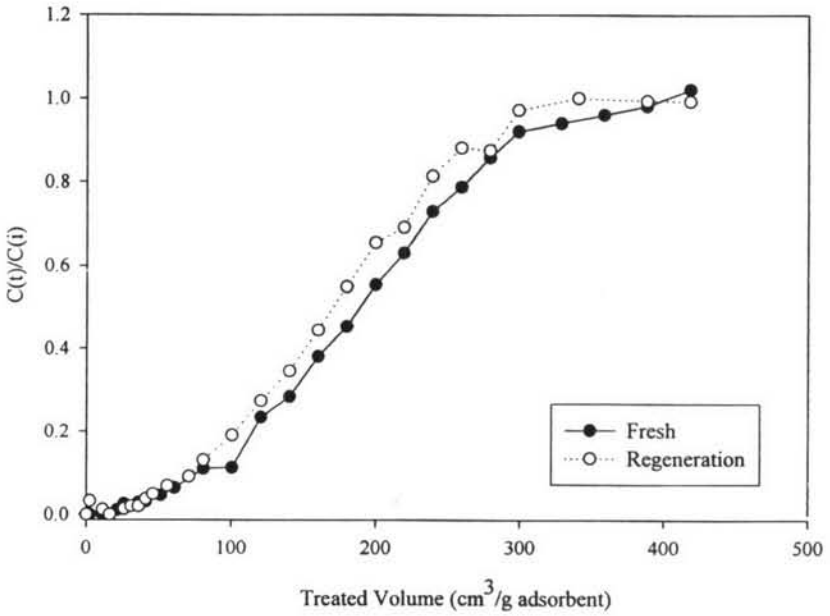

Figure 5.9 The effect of desorption of 3-methylthiophene by heating on NaX capacity (desorption time 3 hrs at 400°C).

Figures 5.10 and 5.11 show the comparison between the adsorption of 1000 ppmw of BT on fresh NaX and regenerated NaX after heating the column for 1 and 3 hours, respectively. After regeneration, it was found that NaX can be recovered only 87.7% and 89.3% of the original adsorption capacities for 1 and 3 hours heating, respectively. It is also observed that the recovered adsorption capacity of NaX adsorbed with BT is lower than that adsorbed with 3-MT (Figures 5.8 and 5.9). The results reveal that it is more difficult to desorb BT from NaX than 3-MT. This may be due to interaction between π-electrons in the benzene ring of BT and acidic surface of the zeolite which is stronger when compared to 3-MT adsorption on the zeolite. For heating time similar results to 3-MT was observed here that is very small difference between heating for 1 hour and 3 hours.

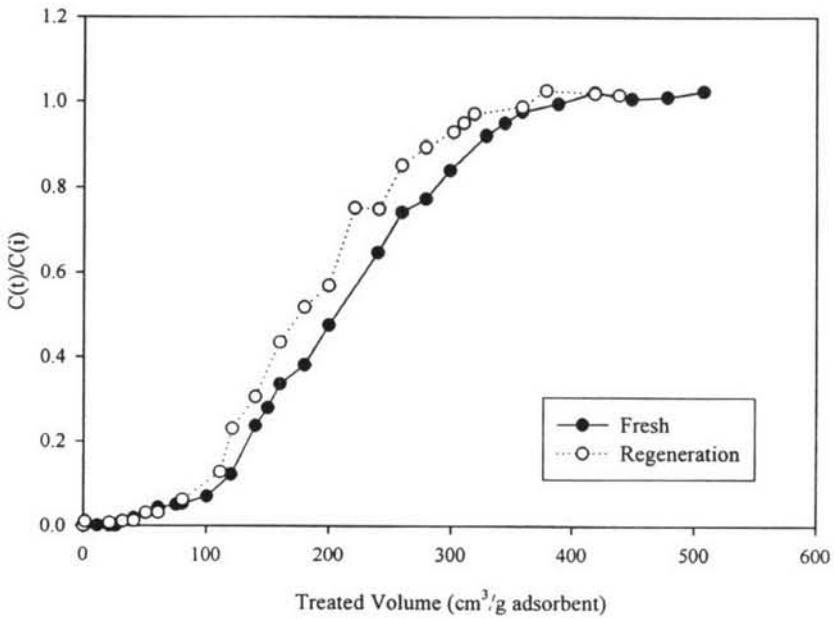

Figure 5.10 The effect of desorption of benzothiophene by heating on NaX capacity (desorption time 1 hr at 400°C).

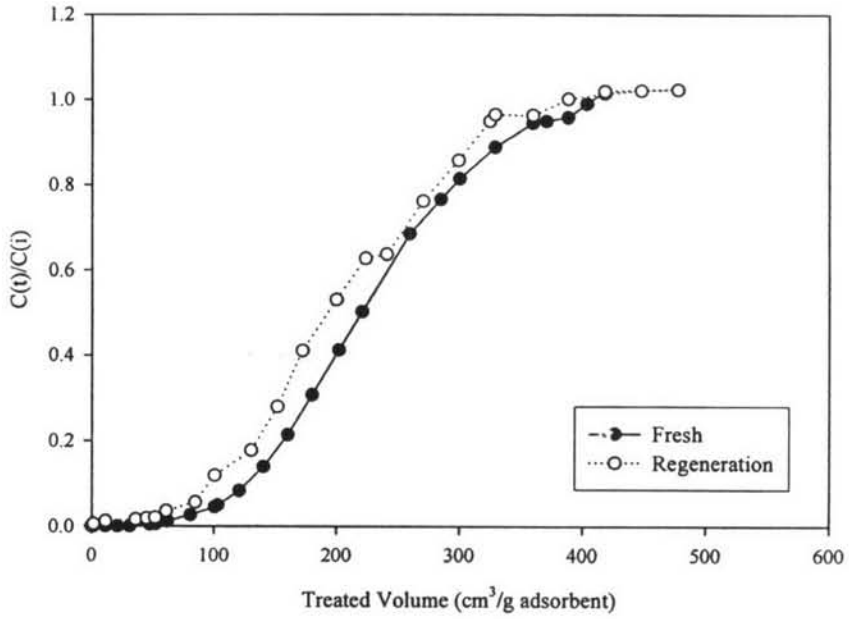

Figure 5.11 The effect of desorption of benzothiophene by heating on NaX capacity (desorption time 3 hrs at 400°C).

Figures 5.12 and 5.13 show the comparison between the adsorption of 1000 ppmw of DBT on fresh NaX and regenerated NaX after heating column for 3 and 6 hours, respectively. From the results, it can be obviously seen that the spent NaX can not be recovered efficiently. This is probably due to the influence of two benzene rings in DBT's structure that can be polarized on zeolite surface, thus forming strong interaction which is very difficult to break. Another reason may be explained by the condensation of DBT vapor in the tube after leaving from the furnace as observed from figure 5.13. From this figure, it can be seen that the effluent sulfur concentration of regenerated NaX is higher than initial sulfur concentration. This is due to the re-dissolving of the condensed DBT into the solution after starting the second cycle of adsorption.

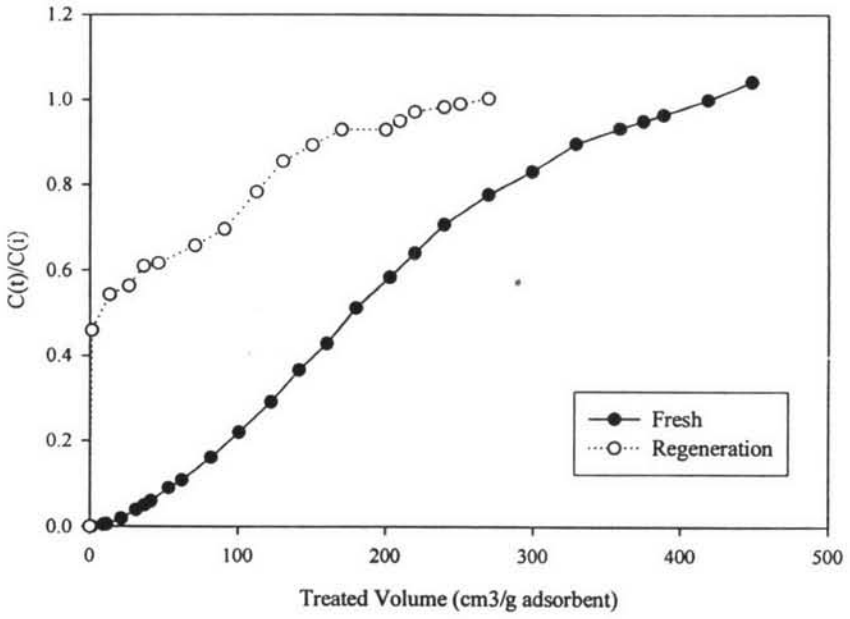

Figure 5.12 The effect of desorption of dibenzothiophene by heating on NaX capacity (desorption time 3 hrs at 400°C).

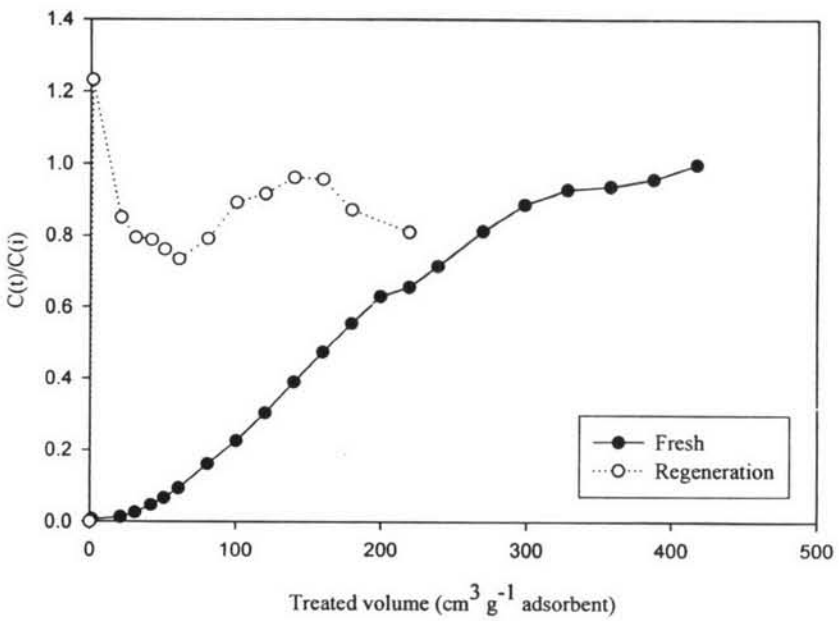

Figure 5.13 The effect of desorption of dibenzothiophene by heating on NaX capacity (desorption time 6 hrs at 400°C).

5.3 Mathematical Models for the Adsorption of Sulfur Compounds on NaX Zeolite

The dynamic adsorption model was developed using both mass transfer and adsorption theories to investigate the adsorption of sulfur compounds from simulated transportation fuels on NaX zeolite. The mathematical model derived from mass balance on liquid phase in the bed and adsorbate in the pellet was used in numerical solving to predict the theoretical breakthrough curve as indicated by following equations.

Mass balance on bulk phase in the bed

$$\frac{\partial c_b}{\partial t} = \frac{D_L}{\varepsilon_b}\frac{\partial^2 c_b}{\partial z^2} - \frac{v_z}{\varepsilon_b}\frac{\partial c_b}{\partial z} - \frac{15(1-\varepsilon_b)K_m D_p (c_b - \bar{c}_p)}{\varepsilon_b R_p^2 (K_m + 5D_p / R_p)} \tag{5.1}$$

Mass balance on adsorbate in the pellet

$$\frac{\partial \bar{c}_p}{\partial t} = -\frac{(c_b - \bar{c}_p)K_m}{(K_m + 5D_p / R_p)\varepsilon_p}\left[\frac{27 D_c K (1-\varepsilon_p)}{R_c^2} - \frac{15 D_p}{R_p^2}\right] \tag{5.2}$$

This model incorporates all resistances to mass transfer, namely: diffusion in the liquid film around the pellets in the bed, diffusion in the binder-phase of zeolites and within the crystals, and adsorption/desorption at the interface of binder-phase and crystals. As described in the mathematical modeling section, the concentration profiles within the zeolite crystal due to radial diffusion in the micropores of crystals was averaged and the adsorption of sulfur compounds at the interface of crystals and macropores was assumed from linear adsorption isotherm. The parameters utilized in the model such as the liquid film mass transfer coefficient around pellet (K_m), dispersion coefficient in the packed bed (D_L) and macro-pore diffusivity (D_p) incorporating the Knudsen effects and molecular diffusivity were either calculated or estimated based on both physical properties of sulfur compounds and adsorbent. The mathematical models for generating breakthrough curve were developed using both MATLAB™ and FEMLAB™ softwares for solving the

governing equation. The model predictions were performed under identical experimental conditions.

5.3.1 Program Testing

In order to predict the theoretical breakthrough curve using MATLAB™ program, the modeling algorithm and programming skill are required. Whereas, FEMLAB™ which is a software package for solving partial differential equations can build this model simply by defining the relevant physical properties rather than defining the algorithm directly. So, the comparison between theoretical breakthrough curve from FEMLAB™ and MATLAB™ was used to verify the accuracy of MATLAB™ algorithm. For these investigations, the experimental breakthrough curves of sulfur compounds were taken a random at every initial concentration as shown in Figures 5.14 to 5.17. These comparisons show that theoretical breakthrough curves from MATLAB™ model were observed to be in good agreement with those from FEMLAB™ model. From the results, it indicates that adsorption model developed using MATLAB™ program can accurately generate theoretical breakthrough curve compared to the commercial software, 'FEMLAB™'.

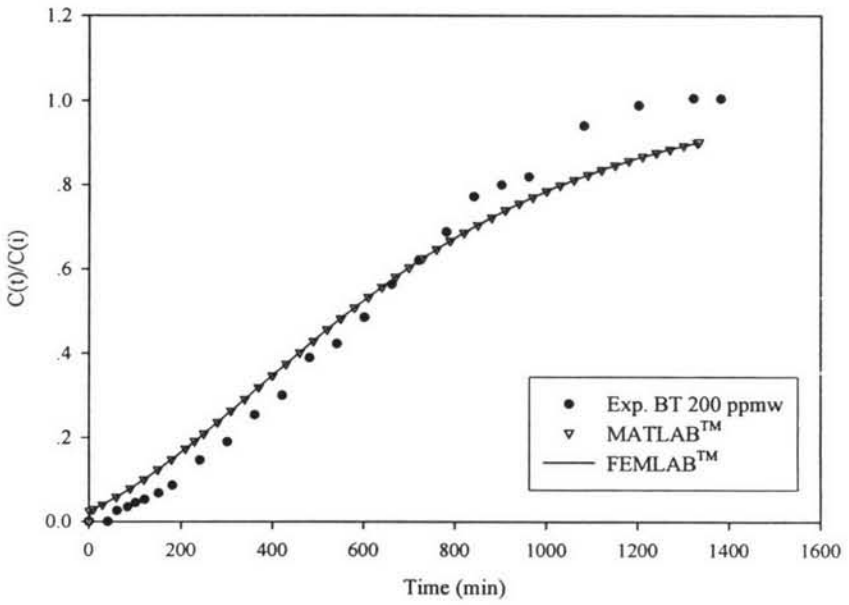

Figure 5.14 Comparison of the mathematical breakthrough curves developed using MATLAB™ and FEMLAB™ at 200 ppmw of BT.

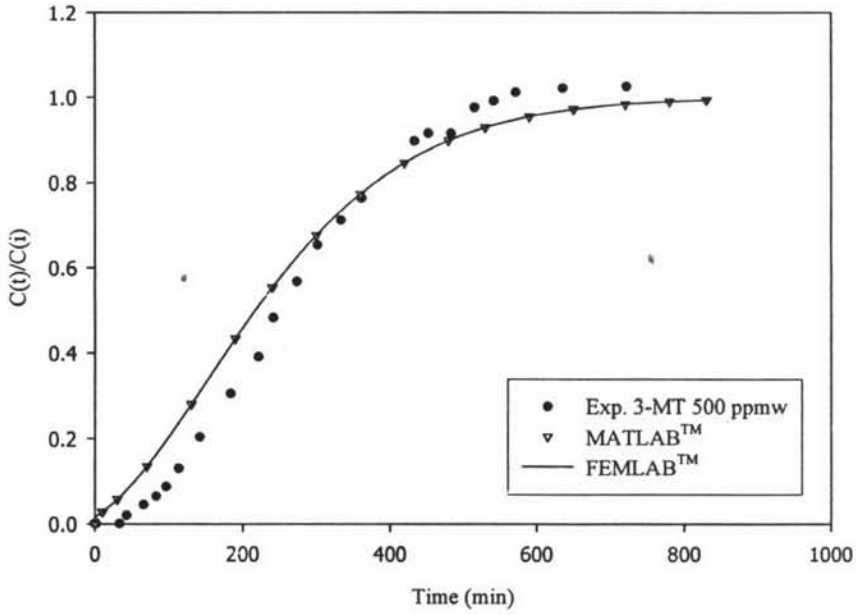

Figure 5.15 Comparison of the mathematical breakthrough curves developed using MATLAB™ and FEMLAB™ at 500 ppmw of 3-MT.

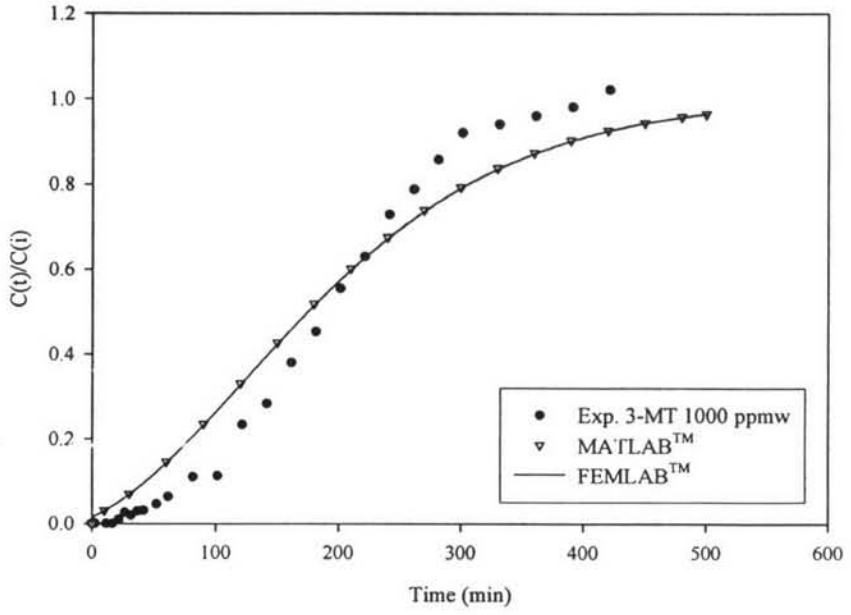

Figure 5.16 Comparison of the mathematical breakthrough curves developed using MATLAB™ and FEMLAB™ at 1000 ppmw of 3-MT.

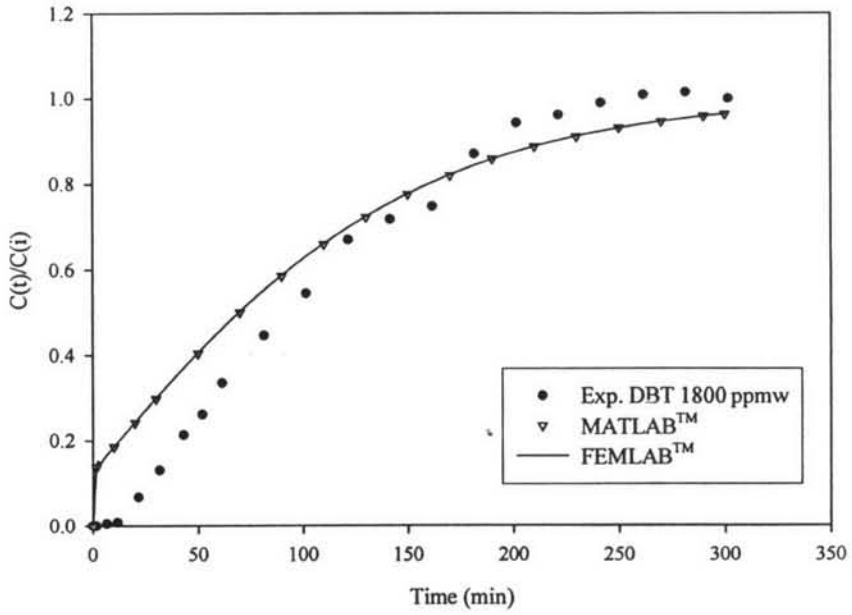

Figure 5.17 Comparison of the mathematical breakthrough curves developed using MATLAB™ and FEMLAB™ at 1800 ppmw of DBT.

5.3.2 Comparison of Experimental and Theoretical Breakthrough Curves

After the comparison of the results from MATLAB™ and FEMLAB™ model, b oth of them provided the same trends of theoretical breakthrough curves. Therefore, FEMLAB™ model was chosen to solve the mathematical model since it reduces computational time. However, once the FEMLAB™ software is not available, MATLAB™ program is able to develop the breakthrough curve although it requires longer computational time. The predicted breakthrough profiles for sulfur adsorption on NaX zeolite under various initial sulfur concentrations were depicted in Figures 5.18 to 5.20.

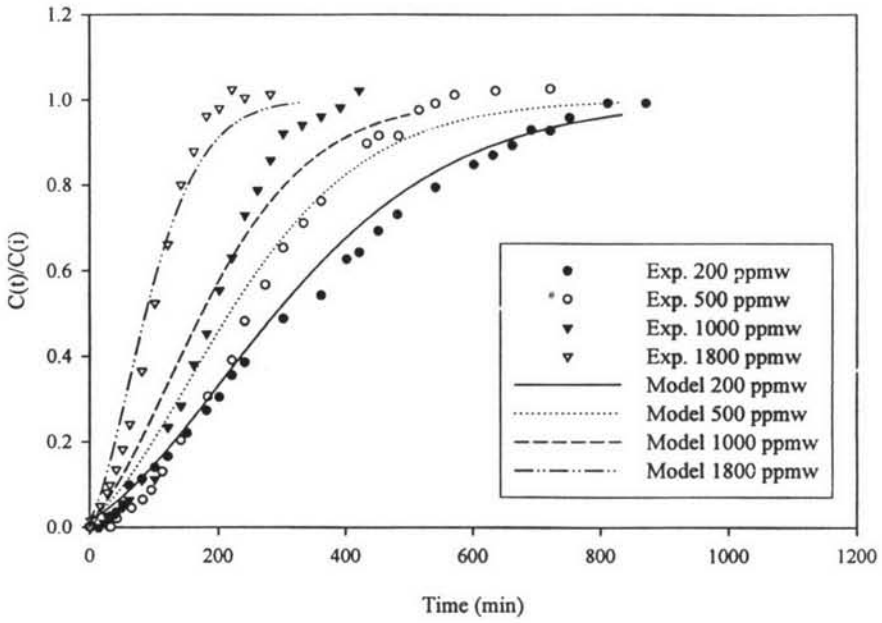

Figure 5.18 Comparison between experimental and mathematical breakthrough curves of 3-MT adsorption on NaX zeolite.

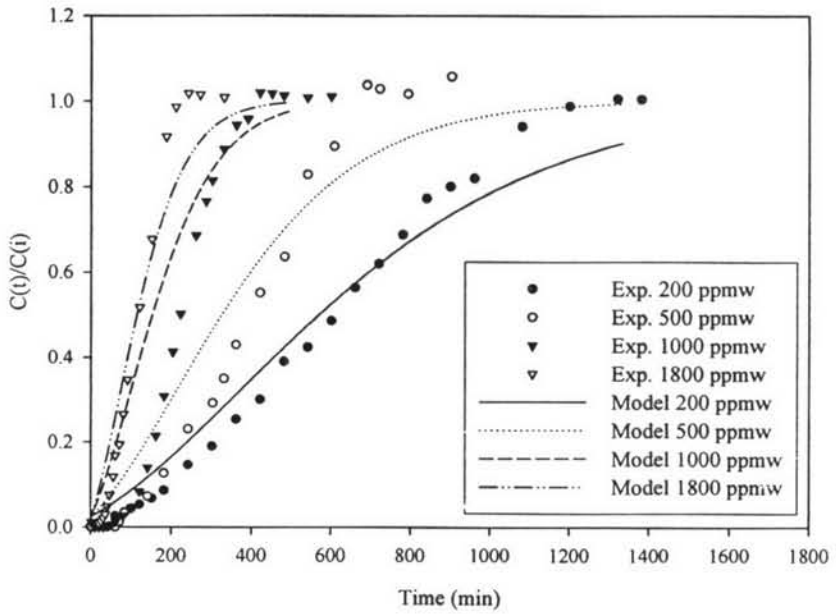

Figure 5.19 Comparison between experimental and mathematical breakthrough curves of BT adsorption on NaX zeolite.

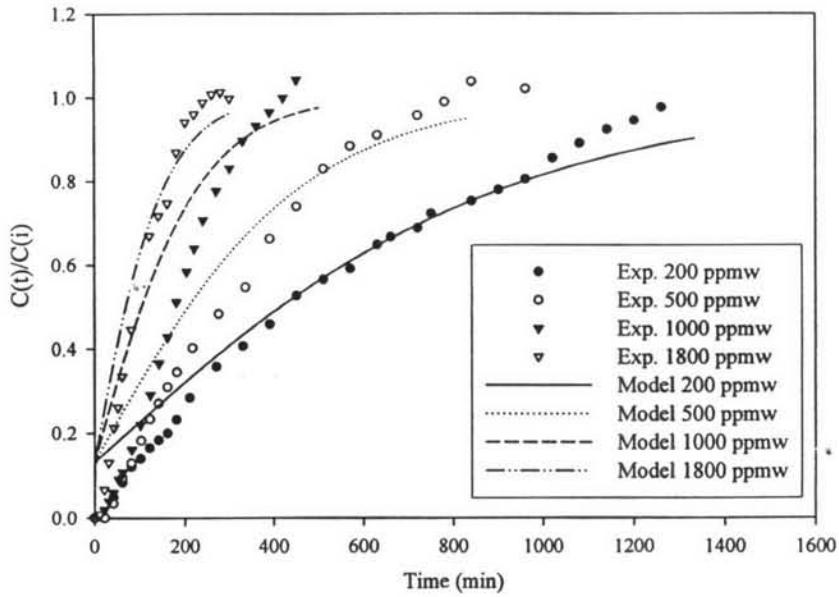

Figure 5.20 Comparison between experimental and mathematical breakthrough curves of DBT adsorption on NaX zeolite.

In order to obtain the best agreement between experimental and mathematical breakthrough curve, the last term of Eq. 5.2 including unknown parameters which are equilibrium coefficient (K), adsorbate diffusivity within the crystal (D_c) and crystal radius (R_c). should be adjusted. This term considered as adjusted parameter describe the rate of sulfur adsorption.

$$Adjusted \quad Parameter(a) = \left[\frac{27 D_c K (1 - \varepsilon_P)}{R_c^2} - \frac{15 D_P}{R_P^2} \right] \tag{5.3}$$

The 'a' values of various conditions were presented in Table 5.3 and also depicted in Figure 5.21. Increase in 'a' value means increase in the adsorption rate. If the adsorption rate is increased, the mass transfer zone which is the region having ability in adsorption is decreased. Therefore, the steeper curve is generated. From the experimental results, it can be observed that the shape of adsorption breakthrough curves of sulfur compounds depends highly on initial sulfur concentration. However, as concentrations increases, the slope of adsorption breakthrough curve dramatically

increases. Consequently, the '*a*' value should be adjusted to higher tendency for higher initial sulfur concentration.

Table 5.3 Adjusted parameters for generating breakthrough curves of sulfur adsorption

Concentration (ppmw)	3-MT	BT	DBT
200	9.0E-05	4.0E-05	2.5E-05
500	1.2E-04	7.0E-05	5.0E-05
1000	1.6E-04	1.4E-04	1.0E-04
1800	3.0E-04	2.0E-04	1.5E-04

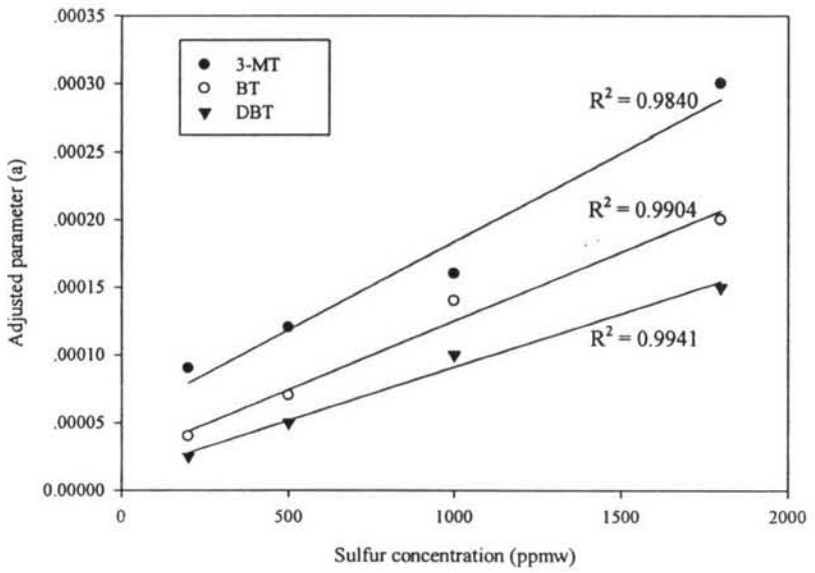

Figure 5.21 The adjusted parameters at various sulfur concentration.

From figure 5.21, it is observed that the trend of '*a*' for each types of sulfur compounds increase in the order of 3-MT>BT>DBT that relate with effective diffusivity value (D_P) as shown in Table 5.4. Normally, the rate of adsorption described in terms of *'a'* is proportional to the diffusion rate. From experimental results shown in figures 5.4 to 5.7, it can be obviously seen that the slope of

breakthrough curve for DBT is the lowest compared to that of 3-MT and BT. This results in the lowest of '*a*' value implied that the adsorption rate of DBT is quite low. This is due to the influence of steric hindrance effect on the diffusion of relatively big molecule like DBT into macro and micro-pores of zeolite. In case of 3-MT and BT, the slopes of 3-MT and BT are not quite different. It can be probably implied that both of them has the similar adsorption rate which is not related to the trend of 'a' value as shown in figure 5.21. The disagreement between the experimental result and the 'a' value from mathematical model may be due to the fact that the terms of interaction that existing in case of BT as described in experimental part was neglected.

Table 5.4 The effective diffusivity of each types of sulfur compounds inside the adsorbent particle

Types of sulfur compounds	Effective diffusivity inside the adsorbent particle (D_P)
3-MT	6.22E-10
BT	5.51E-10
DBT	2.94E-10

From the comparison between the experimental and theoretical breakthrough curve, there are some errors between both of them. It is supposed that the model was correct. The difference between the theoretical and mathematical breakthrough curves at the same conditions could be occurred from the errors in the experiment itself, such as variation of liquid velocity inside the bed and measurement. However, this deviation might occur from the unsatisfied assumption. And also, there were adsorbent and sulfur compound properties estimated from the reference book may cause the error of the theoretical breakthrough curve. These recommendations to accomplish more representative and accurate will be summarized in CHAPTER VI.